J Solid State Electrochem (1998) 2: 405–412

ORIGINAL PAPER

Leonardo Salgado · Hugo Sánchez · Carlos R. Cabrera
Raúl J. Castro · Yunny Meas

Underpotential deposition of Cu on partially oxidized Rh electrodes

Received: 11 July 1997 / Accepted: 10 February 1998

Abstract The underpotential deposition (UPD) of copper on partially oxidized rhodium electrodes was studied in acid medium using potentiodynamic techniques. The process was analyzed as a function of the potential and time of deposition. The potentiodynamic *I-E* patterns for the oxidative dissolution of Cu provide evidence for the existence of a chemical reaction between Cu and oxygen existing on the electrode surface. Redistribution of the active sites is also possible when appreciable quantities of oxidized species are simultaneously reduced by the UPD process. The partially oxidized rhodium electrodes were prepared by cyclic voltammetry and anodic polarization. The later method provided the most oxidized surfaces, but, even in this case, the degree of oxygen surface coverage was lower than that corresponding to a monolayer.

Key words Underpotential deposition · Copper · Rhodium

Introduction

The underpotential deposition (UPD) of foreign metals onto substrates has been widely studied as an important theoretical and applied facet of electrocatalysis [1, 2]. However, few studies have examined the UPD of metals with interference of the oxygen electrosorption process produced on electrodes of the Group VIII metals [3]. On these electrodes, the UPD of a metal can be accomplished with oxygen electroadsorption when the equilibrium potential for the M/M^{n+} redox couple of the metal deposited is sufficiently positive, such that the underpotential deposition of metal interferes with the oxygen electroadsorption, as occurs with the silver-platinum system [4–9], and/or when the oxygen electroadsorption process on the substrate is initiated at relatively low potential values, depending fundamentally on the nature of the substrate [3]. Consequently, the presence of the oxygen species on the electrode surface, due either to simultaneous adsorption of oxygen with the metal UPD or the preparation method of the electrodes before the metal UPD, might have an important influence on the formation of the metal layer. Although this effect has been studied for the silver-platinum system [4–9], it has not been reported for other systems. Understanding the influence of O electroadsorbed on the UPD process of metals is fundamental for clarifying the mechanisms of electrochemisorption and electrocatalysis in these systems.

Rhodium is a metal which, like platinum, is important as an electrocatalyst [10–11]. The UPD process of Cu on platinum electrodes has been widely studied, and its electrochemical behavior is well understood [12–17]. However, for rhodium electrodes, few studies deal with the metallic UPD in relation to platinum, and existing publications are mainly concerned with the study of the UPD of copper processes [18–19]. Some discussions of the effect of the coadsorption of anions on this type of process have been published [20, 21], yet, unlike the Pt/Cu^{2+} system, the Rh/Cu^{2+} system does not exclude the possibility that the UPD process can be affected by the existence of traces of oxide on the Rh surface, as indicated by Parajon et al. [18].

Therefore, the aim of this work is the obtention of partially oxidized rhodium electrodes in order to study

L. Salgado (✉) · H. Sánchez
Area de Electroquímica,
Universidad Autónoma Metropolitana-Iztapalapa,
Apdo. Postal 55-534, México D.F., 09340 México
Tel.: +52-5-724 4670; Fax: +52-5-724 4666
e-mail: lsj@xanum.uam.mx

C.R. Cabrera · R.J. Castro
Department of Chemistry and Materials Research Center,
P.O. Box 23346, Río Piedras Campus,
University of Puerto Rico 00931-3346, Puerto Rico

Y. Meas
Centro de Investigacion y Desarrollo Tecnológico
en Electroquímica, Sanfandila Pedro Escobedo,
Apdo. Postal 064,
Querétaro 76700, México

the effect of the coadsorbed oxygen on the UPD process of copper in acid media.

Experimental

A glass electrochemical cell with three electrodes, suitable for working in a nitrogen atmosphere, was used. The working electrode was a polycrystalline rhodium wire (Johnson Matthey, 99.99%) of 0.164 cm^2 geometric area, previously treated with hot chromic acid followed by thorough washing in triple-distilled water, polished with alumina 5-μm grit, cleaned with HNO_3 + H_2SO_4 and finally rinsed with triple-distilled water. A carbon rod (spectroscopic grade) was used as a counter electrode and the reference was an $Hg/Hg_2SO_4/K_2SO_4$ saturated electrode connected to the cell by means of a Luggin capillary. In this work, all potentials are referenced to the standard hydrogen electrode (SHE).

All experiments were performed at room temperature in 1 M H_2SO_4, prepared from sulfuric acid (Merck AR), and triple-distilled water, deionized with a Millipore system. The deaerated electrolytes satisfied the purity criterion established by the repetitive voltammetric *I-E* response of the Pt/H_2SO_4 (aq) [22].

The working electrode was subjected to triangular potential cycling between 0.05 and 0.96 V at 40 mV s^{-1} until no changes occurred in the voltammogram (~20 cycles). The real surface area of the rhodium electrode was determined by hydrogen adsorption according to [23], and the roughness factor, f_r, was calculated ($f_r = 8.52$).

The oxidized rhodium electrodes were prepared in two ways: (1) by application of a triangular potential scan until a constant *I-E* pattern was obtained and (2) by anodic polarization of the electrode for a constant time, t_{ox}. Details of these procedures are described below. Surface oxides of the rhodium electrode were characterized by cyclic voltammetry in 1 M H_2SO_4. Two conditions of the degree of surface oxidation were obtained, and both imply a partial oxidation of the electrode; these are the working surfaces used to study the UPD process of copper.

The partially oxidized rhodium electrodes were prepared *in situ* using a working solution of 1 M H_2SO_4 + 4.2×10^{-4} M $CuSO_4$ (Merck AR). The electrodes were used immediately to analyze the UPD process of copper.

The UPD process of copper was studied as a function of time at a constant potential. The effect of the oxide is discussed from the *I-E* potentiodynamic profiles (40 mV s^{-1}) for the oxidative dissolution of copper adatoms.

A PAR 273 potentiostat was used. The presence of oxidized species on the electrode surface was corroborated with electron spectroscopy for chemical analysis (ESCA), done with a PHI 5600 ci, using Mg Kα (15 kV, 400 W) radiation source, a concentric hemispherical analyzer operating in a fixed transmission mode, and a multichannel detector. The operating pressure of the system was better than 5×10^{-9} torr, and the take-off angle for the photoelectrons was 45°. Survey spectra were acquired with a 93.9-eV pass energy. The analysis area for all measurements was 700 μm. High-resolution multiplex spectra were recorded using pass energy of 11.750 eV. At least five scans were done for each energy region. Binding energy was referenced to the C(1 s) line at 284.8 eV to correct for any shift due to charging. The samples were analyzed before and after the sputtering process. An Ar^+ ion gun at a current of 25 nA and a gas pressure of 4 mPa was used for the sputtering process.

Results and discussion

Methodology for the copper UPD process on partially oxidized rhodium electrodes

Oxidation of the electrode surface and subsequent copper deposition were carried out in 1 M H_2SO_4 + 4.2×10^{-4} M $CuSO_4$ by the application of the polarization routines shown in Fig. 1. The rhodium electrode in 1 M H_2SO_4 was subjected previously to a repetitive triangular potential sweep between 0.05 and 0.96 V, at 40 mV s^{-1} for several cycles in order to obtain reproducible and comparable responses. According to diagram a of Fig. 1, the surface oxidation is produced during the anodic scan between the values E_l (lower limit) and E_u (upper limit), while in diagram b of Fig. 1 the surface oxidation is produced by anodic polarization at the E_u potential during the oxidation time t_{ox}. These oxidation procedures produced different degrees of surface oxidation despite the E_u potential being the same in both cases, 0.96 V. The lower limits of potential were fixed at two values, 0.42 and 0.32 V, to study the copper UPD process.

Electrochemical characteristics of partially oxidized rhodium electrodes

Figure 2 shows the two potentiodynamic *I-E* profiles for a rhodium electrode in 1 M H_2SO_4 in the potential range 0.32–0.96 V, recorded at 40 mV s^{-1} potential scan rate. Curve a is the stabilized *I-E* response obtained from repetitive triangular potential scans (~20 cycles), and curve b is the *I-E* response for a potential scan after polarization of the electrode at E_u for 20 min, as indicated in Fig. 1. The polarization time was selected from several experiments at different oxidation times, and the

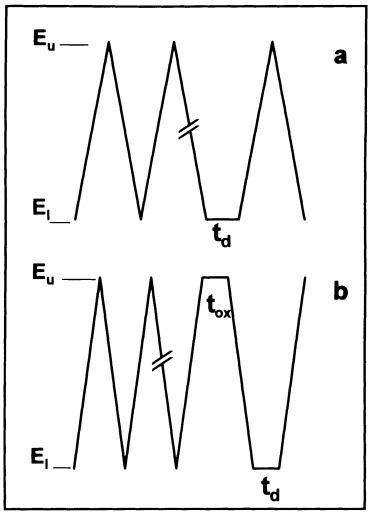

Fig. 1 Potential-time patterns used to prepare the working electrodes: *a* triangular potential sweep and *b* anodic polarization

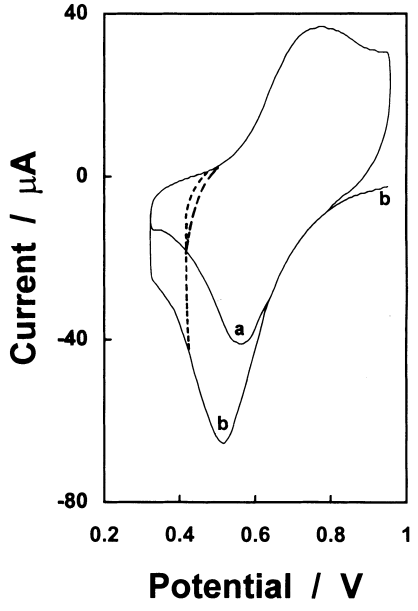

Fig. 2 Voltammograms of rhodium electrodes in 1 M H_2SO_4 at 40 mV s^{-1}: *a* cyclic voltammetry and *b* linear potential scan after anodic polarization

I-E response in Fig. 2 (curve b) corresponds to the minimum time needed to obtain the maximum cathodic peak current.

The *I-E* curves in Fig. 2 show a wide anodic peak between 0.5 and 0.96 V caused by the formation of oxidized species of rhodium on the electrode surface without interference of oxygen evolution since E_u was not sufficiently positive [23–25]. Furthermore, a wide cathodic peak starting from 0.8 V is observed and attributed to the electrochemical reduction of the oxidized species [23–25]. Similar behavior is observed when the lowest potential limit was placed at 0.42 V (dashed curves in Fig. 2).

Comparison of the cathodic *I-E* curves in Fig. 2 shows that potentiostatic anodic polarization (Fig. 2, curve b) produces a cathodic peak current approximately 50% higher than that obtained by cyclic voltammetry, and the peak potential is displaced about 50 mV to less positive potentials. This clearly indicates that anodic polarization produces the highest degree of oxidation of the surface and that the Rh-oxygen species thus formed are more stable than those generated by cyclic voltammetry [24].

The amount of oxide on the electrode surface was indirectly estimated by measuring the charge Q_{red} of each cathodic peak in Fig. 2. From curve a, Q_{red} is 0.23 mC, and from curve b, Q_{red} is 0.39 mC. The oxygen surface coverage of the rhodium electrode was evaluated using the equivalence between Q_{red} and $2Q_{H,s}$ [23], where $Q_{H,s}$ is defined as the monolayer hydrogen charge, and one hydrogen atom is assumed to be adsorbed on one surface metal atom [26]. The values obtained for oxygen surface coverage were 0.40 and 0.68 for the electrodes of curves a and b, respectively.

From these results, two conditions of partial surface oxidation were established, denoted here as PORh[a] and PORh[b]. PORh[a] corresponds to the partially oxidized rhodium electrode obtained by cyclic voltammetry (diagram a, Fig. 1), and PORh[b] corresponds to the electrode prepared by anodic polarization (diagram b, Fig. 1). Electron spectroscopy for chemical analysis (ESCA) measurements showed that the oxygen contents on the two electrodes are in the same ratio as that previously determined from the Q_{red} data. These were the base surfaces to study the copper UPD process.

Copper UPD process on PORh[a] and PORh[b]

The UPD process of copper on PORh[a] and PORh[b] was studied as a function of the deposition time (t_d, Fig. 1) at two fixed potentials, 0.42 and 0.32 V. The potentiodynamic *I-E* profiles for the oxidation and dissolution of Cu adatoms are discussed separately for each applied deposition potential.

UPD of copper on PORh[a] and PORh[b] at $E_d = 0.42$ V

When the applied deposition potential was 0.42 V and at low values of t_d, the potentiodynamic *I-E* profiles for the oxidation of Cu from PORh[a] (Fig. 3a) and PORh[b] (Fig. 3b) showed only an anodic peak at 0.58 V, which is attributed to the oxidation and desorption of strongly adsorbed Cu adatoms [18]. The evolution of the oxidation peak with changing t_d is similar for both types of electrodes, i.e., the anodic peak current increased when t_d was raised and the maximum peak current was obtained when t_d was 360 s for PORh[a] and 900 s for PORh[b] without changes in the peak potential value. The additional increment of t_d produced significant changes in the *I-E* pattern: the oxidation peak current decreased and the corresponding peak potential was displaced to more positive values, indicating that the Cu adatoms are in a more stable energy state than those formed at the lowest t_d values.

These results show that the UPD process of copper follows a typical behavior pattern [1, 15, 16, 27, 28] on PORh[a] and PORh[b] at relatively low values of t_d. However, at the highest t_d values the electrochemical behavior of the oxidation peak differs from that reported for the same adsorbate [15–19, 26–28]. Therefore, the UPD process on both types of electrodes starts on equivalent active sites, but the subsequent deposition steps (high t_d values) involve the formation of more stable adsorbed species.

Because of the metallurgical properties of these metals [29], obtaining very stable species of Cu UPD could be due to a penetration effect of Cu into the rhodium electrode. D.W. Goodman [30], however, studied the interaction between ultrathin copper films and Rh (100) by XPS and found no evidence for the formation of rhodium-copper alloys. Because our experiments were of

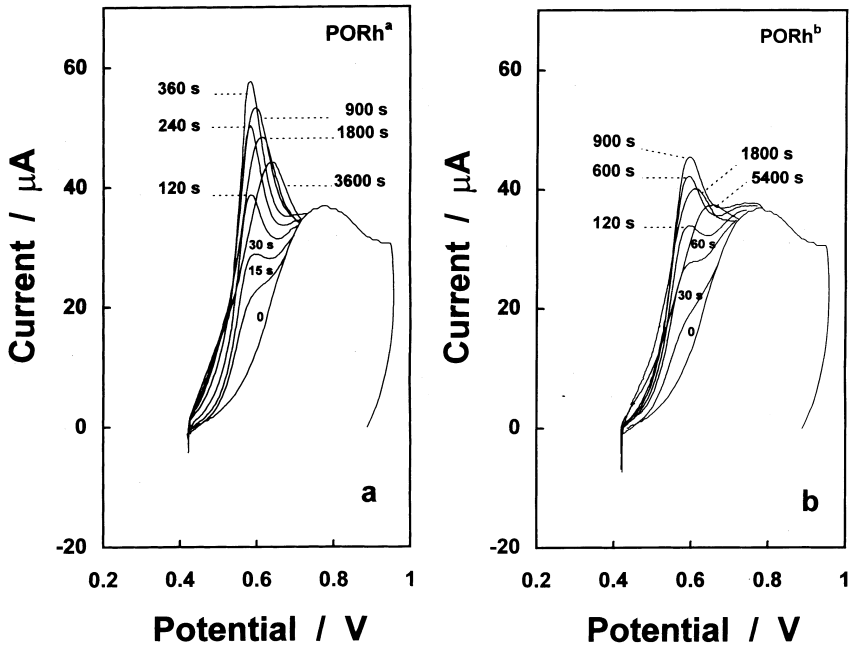

Fig. 3 Anodic potential scan (40 mV s^{-1}) of PORh[a] (**a**) and PORh[b] (**b**) electrodes after UPD of copper at E_d = 0.42 V and various deposition times

relatively short duration, the production of Cu-Rh alloys was unlikely.

After correcting for surface oxidation, the integral under the oxidation peaks in Fig. 3a and b allowed us to evaluate the electric charge due to the desorption process of copper adatoms (Q_{Cu}). Variation of Q_{Cu} with respect to t_d for PORh[a] and PORh[b] is given by curves a and b in Fig. 4, respectively. When t_d was smaller than 300 s, the increase in Q_{Cu} was faster in PORh[a] than in PORh[b], indicating that in PORh[a] the amount of active sites

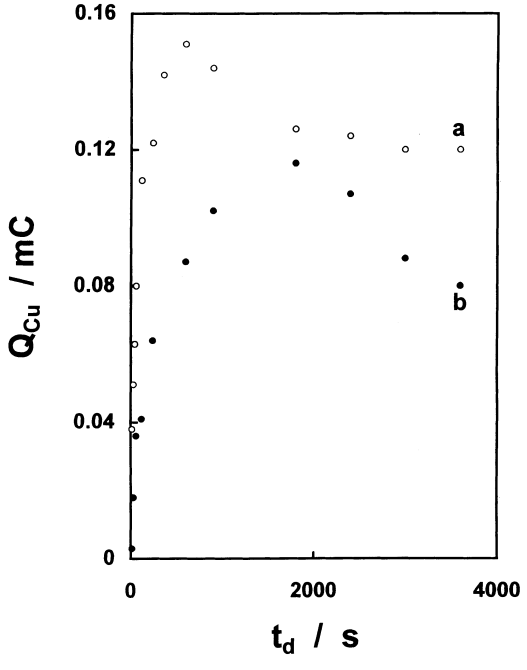

Fig. 4 Q_{Cu} vs t_d graph for PORh[a] (**a**) and PORh[b] (**b**) electrodes; E_d = 0.42 V

available for copper adsorption is higher than in PORh[b]. This is expected since PORh[b] is the more oxidized electrode. In both curves (Fig. 4) a maximum was observed at 0.143 mC (t_d = 600 s) for PORh[a] and 0.102 mC (t_d = 1800 s) for PORh[b], demonstrating that in PORh[b] the density of active sites is lower than in PORh[a]. These results indicate that the oxidized species remain on the electrode surface in spite of the t_d and deposition potential applied. From the maximum observed in Fig. 4 and the equivalence between Q_{Cu} and $2Q_{H,s}$ [31], the degree of surface coverage by Cu adatoms was evaluated: 0.26 for PORh[a] and 0.20 for PORh[b]. The lower value was as expected for PORh[b], since this electrode is more oxidized than PORh[a].

A decrease in Q_{Cu} was observed in Fig. 4 for the highest t_d values. The decrease was 17% for PORh[a] (in relation to the maximum value) and the curve flattened to a constant value from t_d = 1800 s. However, in PORh[b] the drop in Q_{Cu} was continuous even after t_d = 3000 s. It is important to emphasize that Q_{Cu} in PORh[a] was always higher than in PORh[b] for the applied t_d values in this set of experiments.

These results show that the adsorbed oxygen on the electrode surface is only partially reduced during the copper UPD process. However, to corroborate the coexistence of Cu and oxygen on the electrode surface, ESCA measurements were performed. For these measurement, the PORh[a] and PORh[b] electrodes were used after UPD copper deposition at E_d = 0.42 V for the most extreme condition of t_d, i.e. 3600 s. The corresponding spectra gave evidence for the coexistence of Cu and oxygen on both types of electrodes, as illustrated by the ESCA spectrum of Cu/PORh[a] in Fig. 5.

The decrease in Q_{Cu} when t_d was high observed in both oxidized electrodes (Fig. 4) could be due to the chemical interaction between the copper adatoms and

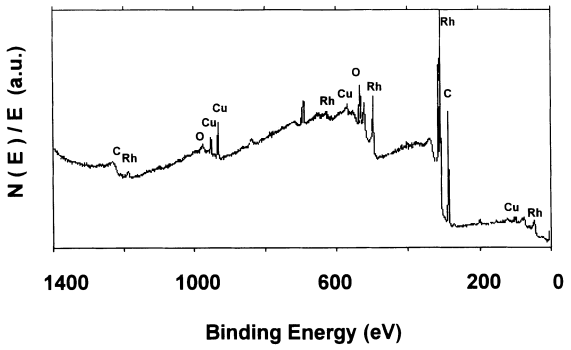

Fig. 5 ESCA survey spectrum (Mg Kα) for Cu/PORh[a]

the oxygen existing on the electrode surface. As recently discussed, the coexistence of copper and oxygen on the electrode surface produces the chemical reaction [32]

$$2Cu_{ads} + \frac{1}{2}O_{2,ads} \rightarrow (Cu_2O)_{ads} \quad (1)$$

which takes place simultaneously with the UPD process of copper

$$Cu^{2+} + 2e^- \rightarrow Cu_{ads} \quad (2)$$

Chemical reaction 1 implies the existence of Cu^+ as well as Cu° on the electrode surface. When the potential scan is applied in the anodic direction, the total current is due to the oxidation of both copper species and the oxidation of rhodium, whose contribution is eliminated. For the lowest t_d values, the total charge of the oxidation of copper to obtain Cu^{2+} is practically due to the oxidation of Cu°. However, when t_d is increased, the quantity of Cu^+ increases, and, therefore, the total charge of the dissolution process decreases, as shown in Fig. 4. This effect is more important for the PORh[b] than for the PORh[a] electrode since it is the more oxidized of the two. The observed displacement of the peak potential to more positive values in Fig. 3 for the highest t_d values can be justified by the existence of chemical reaction 1, which provides more stable chemical species.

UPD of copper on PORh[a] and PORh[b] at $E_d = 0.32$ V

When the applied deposition potential was 0.32 V, the potentiodynamic *I-E* profiles for the oxidation of Cu adatoms from PORh[a] (Fig. 6a and b) and PORh[b] (Fig. 7a and b) showed two peaks at 0.48 V (peak I) and 0.58 V (peak II). These are normally attributed to the oxidation of weakly and strongly adsorbed Cu adatoms, respectively [18].

The shape of peaks I and II, as a function of the applied t_d, was influenced significantly by the surface condition of the electrode. In PORh[a] (Fig. 6a), peak II was clearly observed from $t_d < 60$ s, while peak I was present only from $t_d = 120$ s. The heights of peaks increased as t_d increased, and peak II was the highest for all the applied values of t_d (Fig. 6b). This indicates that the UPD process of copper takes place mainly on high-energy active sites, but, also, at the same time, on lower-energy active sites (peak I). The maximum current for peak II was reached when $t_d = 360$ s, while the region of peak I showed a continuous increase up to a certain point and there reached a plateau from $t_d = 1800$ s. When $t_d > 360$ s, peak II decreased and showed a slight displacement to more positive potentials (Fig. 6b).

The integral under the curves in Fig. 6a and b is shown in Fig. 8 (curve a) as a function of t_d. In this case, the charge due to the electrodissolution of copper

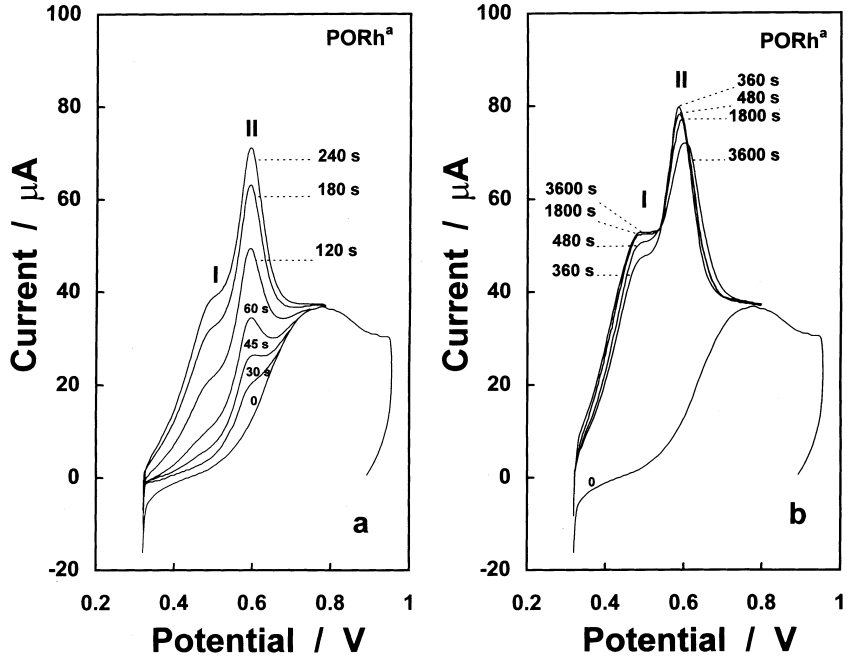

Fig. 6 Anodic potential scan of PORh[a] electrode after UPD of copper at $E_d = 0.32$ V for low (**a**) and high (**b**) deposition times

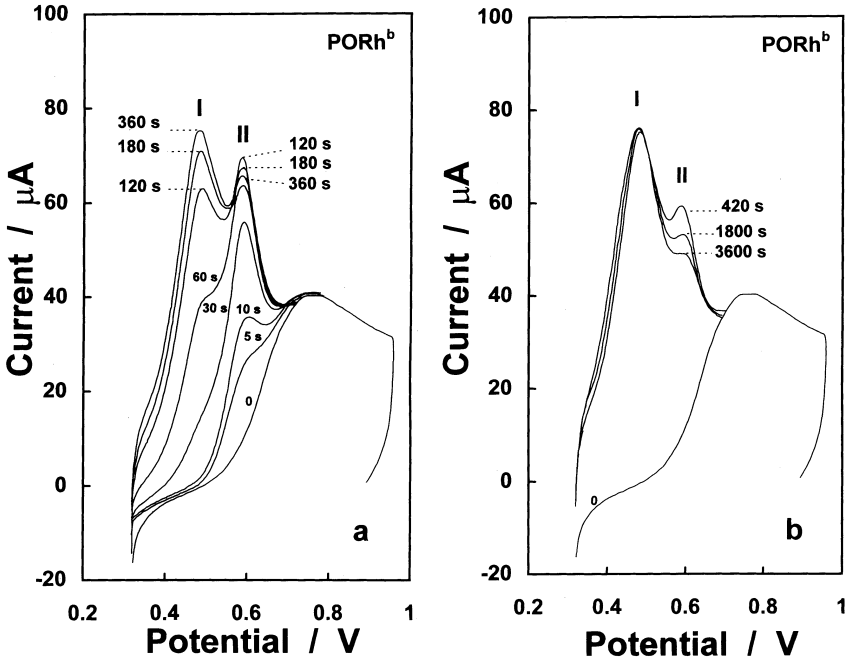

Fig. 7 Anodic potential scan of PORh[b] electrode after UPD of copper at $E_d = 0.32$ V for low (**a**) and high (**b**) deposition times

adatoms from PORh[a] was practically constant from $t_d = 900$ s. However, when t_d was 360 s, the electric charge had not yet reached its maximum value, and the observed increase was due to the UPD process taking place only on low-energy active sites (peak I). Therefore, the observed decrease in peak II from $t_d = 360$ s can be attributed to a surface rearrangement of the substrate which promotes active sites to be transformed from high energy to low energy. This is an additional effect that favors the growth of the current in peak I. Consequently, the total quantity of copper deposited through UPD is reached at high values of t_d (>900 s), when the low and high energy active sites have been occupied by the copper adatoms and only after the surface rearrangement has concluded. Application of a t_d higher than 3600 s did not lead to a major decrease in peak II (Fig. 6b), demonstrating that the surface rearrangement was already completed. In this case, the possibility of surface diffusion of the copper adatoms to the low-energy active sites can be disregarded, since such diffusion would be incapable of producing the observed decrease in peak II current (Fig. 6b). This interpretation is reinforced by the results obtained for the PORh[b] electrode which are described below.

For the PORh[b] electrode (Fig. 7a and b), peaks I and II showed a gradual variation of peak current as t_d was varied. Initially, only growth of peak II was observed ($t_d < 60$ s) and peak I appeared only for $t_d \geq 60$ s. When $t_d \leq 120$ s, peak II was higher than peak I, but the opposite was observed when $t_d > 120$ s (Fig. 7a). The maximum current of peak II was achieved for $t_d = 120$ s, and a higher t_d led to a gradual decrease of this peak. For peak I, the maximum current was obtained for $t_d = 360$ s (Fig. 7a), and this current and peak potential remained unchanged when a higher t_d was applied (Fig. 7b). However, peak II gradually decreased, eventually to a plateau, as observed in Fig. 7b.

The observed behavior of the oxidation peaks I and II as a function of t_d in Fig. 7a and b indicates that the UPD process of Cu on the PORh[b] electrode takes place initially on high-energy active sites, as mentioned above. When t_d was increased, peak I appeared (Fig. 7a) and the UPD process occurred simultaneously on high- and low-energy active sites. The peak potentials for peaks I and II are the same as observed in Fig. 6a and b, indicating that the active sites are equivalent on the two types of electrodes. Again, a decrease in peak II, previously attributed to a surface rearrangement of the substrate, was observed for $t_d > 120$ s. In this case, however, the growth of peak I is very important, as this peak is finally higher than peak II, indicating that, for the PORh[b] electrode, there are more low-energy than high-energy active sites. This result can be a consequence of the exhaustive oxidation of the electrode at E_u and the subsequent reduction of the oxidized species during the UPD process at an E_d value less positive than the one applied in the case of Fig. 3a and b. In addition, the surface rearrangement process indicates a decrease in the quantity of high-energy active sites, and, as the total charge due to the dissolution process of copper is practically constant (Fig. 8, curve b), such a phenomenon promotes the transformation of high- to low-energy active sites.

Evidence of the increase of low-energy active sites on a rhodium electrode due to the reduction of oxidized species has been obtained by Parajon et al. [18], but was not recognized by these authors. The existence of this phenomenon is revealed by comparison of Fig. 2 with Fig. 3 in [18]. In the same reference, the surface rearrangement process is not clear, since it can only be

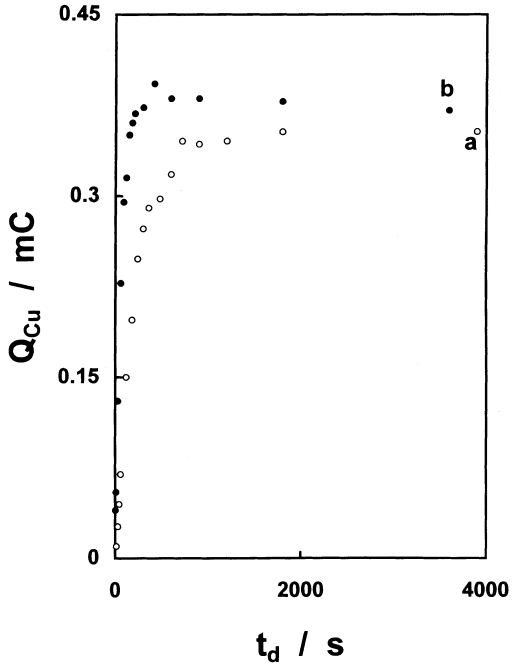

Fig. 8 Q_{Cu} vs t_d graph for PORh[a] (**a**) and PORh[b] (**b**) electrodes; $E_d = 0.32$ V

confirmed from the development of peak II when sufficiently high t_d values are applied, as we report here. We describe how prior oxidation of the electrode (PORh[b]) provided a significant quantity of oxide which, by reduction during the UPD process, led to a predominance of low-energy active sites. This predominance of low-energy active sites is evidenced by the observation that peak I is higher than peak II only at high t_d values. However, as peak II is highest at low t_d values, we must ascribe this effect to kinetic influences.

The variation of Q_{Cu} as a function of t_d for PORh[b] ($E_d = 0.32$ V) is shown in Fig. 8. For this electrode (Fig. 8, curve b), Q_{Cu} increased as t_d was increased, and a maximum of 0.39 mC was obtained. However, for the PORh[a] electrode, the charge only increased up to 0.34 mC. In addition, for all the applied values of t_d, Q_{Cu} values in PORh[b] were higher than the corresponding values in PORh[a]. This proves that the total quantity of active sites for Cu adsorption on PORh[b] was higher than on PORh[a], since both electrodes have the same geometric area and reduction of the more oxidized electrode (PORh[b]) would provide a slightly rougher surface. The degree of coverage of the rhodium surface by copper adatoms was 0.59 in PORh[a] and 0.68 in PORh[b], indicating a coverage degree lower than a monolayer. These values are higher than those previously obtained when the UPD process was performed at 0.42 V.

The curves shown in Fig. 8 imply higher charge quantities than the corresponding curves in Fig. 4, since in Fig. 4 the electrodes (where, additionally, reaction 1 takes place) were partially blocked by oxidized species. In Fig. 8 the electrodes were subjected to a fairly strong reduction, sufficient to produce the classical effect of a UPD process, i.e., where a plateau in the Q vs t_d graph was obtained. We can therefore assume that the oxidized species, initially present on the electrode surface, were almost completely reduced during the copper UPD process.

According to thermodynamics, the UPD process is initially preferential for high-energy active sites, regardless of the oxidized or reduced state of the surface, producing the corresponding peaks in the potentiodynamic diagram without potential variation and indicating unaltered work function. Only at high UPD times is it possible to observe the effects of a chemical reaction and/or a surface rearrangement by means of the electrochemical behavior of the dissolution peaks generated by the adsorbed species.

Conclusion

The presence of oxidized species on the rhodium electrode surface caused important effects on the copper UPD process. In this work, the UPD process was performed simultaneously with reduction of the oxidized species, and such reduction was partial or total. In the case of partial reduction, the remaining oxidized species provoked a blocking effect on the electrode surface that led to low values of degrees of coverage; besides, a chemical reaction on the electrode surface is possible. On the other hand, when the reduction of the oxidized species was completed simultaneously with the UPD process, it caused a redistribution process of the active sites and favored the formation of the low-energy active sites, of which there has not previously been clear evidence. In consequence, the corresponding peak in the potentiodynamic diagram showed an important increase, and such a peak can become higher than the dissolution peak, corresponding to the strongly adsorbed species.

Acknowledgements We would like to thank CONACYT for financial support in the development of this study. C.R.C. and R.J.C. would like to acknowledge the financial support of NSF.

References

1. Kolb DM (1978) In: Gerischer H, Tobias CW (eds) Advances in Electrochemistry and Electrochemical Engineering, vol 11. Wiley, New York, pp 125–271
2. Andricacos PC, Krishnan M, Rath DL (1986) In: Romankiw LT (ed) Proceedings of the symposium on electrodeposition technology, theory and practice, vol 87-17. The Electrochemical Society, Pennington, NJ, pp 449–465
3. Wood R (1977) In: Bard AJ (ed) Electroanalytical chemistry, vol 9. Arnold Press, London, p 1
4. Tindall GW, Bruckenstein S (1971) Electrochim Acta 16: 245
5. Stucki S (1977) J Electroanal Chem 80: 375
6. Ommar FE, Durand R, Faure F (1984) J Electroanal Chem 160: 385

7. Chierchie T, Mayer C, Jüttner K, Lorenz WJ (1985) J Electroanal Chem 191: 401
8. Chierchie T, Milchev A (1990) Electrochim Acta 35: 1873
9. Vaskebich A, Rosenblum M, Gileadi E (1995) J Electroanal Chem 383: 167
10. Goodman DW, Peden CHF, Fisher GB, Oh SH (1993) Catal Lett 22: 271
11. Ross PN, Vinoshita V, Scarpellino AJ, Stonehart PJ (1975) J Electroanal Chem 59: 177
12. Breiter MN (1967) J Electrochem Soc. 114: 1125
13. Bowles BJ (1970) Electrochim Acta 15: 589
14. Tindall GW, Bruckenstein S (1968) Anal Chem 40: 1051
15. Cadle SH, Bruckenstein S (1971) Anal Chem 43: 932
16. Furuya N, Motoo S (1976) J Electroanal Chem 72: 165
17. Margheritis D, Salvarezza RC, Giordano MC, Arvía AJ (1987) J Electroanal Chem 229: 327
18. Parajon B, Pallota CD, De Tacconi NR, Arvía AJ (1983) J Electroanal Chem 145: 189
19. Lapa AS, Safanov VA, Mansurov GN, Petrii OA (1983) Sov Electrochem 19: 502
20. Horanyi G, Wasberg M (1996) J Electroanal Chem 431: 161
21. Shingaya Y, Ito M (1994) J Electroanal Chem 372: 283
22. Conway BE, Angerstein-Koslowska N, Criddle E (1973) Anal Chem 45: 133
23. Rand DAJ, Woods R (1971) J Electroanal Chem 31: 29
24. Pallota C, De Tacconi NR, Arvía AJ (1981) Electrochim Acta 26: 261
25. Chialvo AC, Triacca WE, Arvía AJ (1987) J Electroanal Chem 237: 237
26. Woods R (1974) J Electroanal Chem 49: 217
27. Maksimov YM, Lapa AS, Podlovchenko VI (1989) Sov Electrochem 25: 634
28. Machado SAS, Tanaka AA, Gonzalez ER (1991) Electrochim Acta 36: 1325
29. Massalski TB (1987) Binary alloy phase diagrams, vol 1. American Society for Metals, Ohio, pp 953–954
30. Rodriguez JA, Campbell RA, Goodman DW (1991) J Phys Chem 95: 2477
31. Furuya M, Motoo S (1980) J Electroanal Chem 107: 159
32. Durand R, Faure R, Aberdam D, Salem C, Tourillon G, Guay D, Ladouceur M (1992) Electrochim Acta 37: 1977